Pyrazole *N*-methylide radical cation: ion–molecule reactions in a new hybrid tandem mass spectrometer and DFT molecular orbital calculations†

Robert Flammang,[1]* **Monique Barbieux-Flammang,**[1] **Yves Van Haverbeke,**[1] **Alberto Luna**[2] **and Jeanine Tortajada**[2]

[1]Laboratoire de Chimie Organique, Université de Mons-Hainaut, Avenue Maistriau 19, B-7000 Mons, Belgium
[2]Laboratoire de Chimie Organique Structurale UMR 172, Université Pierre et Marie Curie, Place Jussieu 4, Boîte 45, 75252 Paris Cedex 05, France

ABSTRACT: The gas-phase reactivity of the classical ionized *N*- or *C*-methylpyrazoles and the corresponding distonic pyrazolium *N*-methylide ions **a** and distonic-like pyrazolium *C*-methylide ions **b**, generated from several pyrazole derivatives, was investigated through the use of mass spectrometric techniques and a density functional theory (B3LYP DFT) approach. The calculations performed at the B3LYP/6–311 + G(3df, 2p)//B3LYP/6–31G(d,p) + ZPE level showed the higher stability of the isomers **a** and **b** ions compared with the classical ionized *N*- or *C*-methylpyrazoles. In the light of the theoretical results, the loss of a neutral methylene group from ions **a** and **b** was predicted to be energetically disfavoured, in agreement with experimental findings. Ion–molecule reactions performed in a new hybrid mass spectrometer of sectors–quadrupole–sectors (EBEqEBE) configuration, were used for the characterization of the $[C_4H_6N_2]^{\cdot+}$ ions studied. The targets used were nitric oxide, dimethyl disulphide, dimethyl diselenide, pyridine and acetonitrile. In the specific case of ions **a**, generated from *N*-acetylpyrazole, the presence in the mass spectra (or in the collisional activation mass spectra of mass-selected ion–molecule reaction products) of CH_2NO^+, $CH_3SCH_2^+$ or $CH_3CNCH_2^{\cdot+}$ fragment ions confirms the presence of the CH_2 moiety and therefore their distonic character. The most stable ions **b** proposed to be produced from 3(5)-*N*,*N*-dimethyl-aminopyrazole do not show the same reactivity (i.e. the CH_2 moiety transfer). Because all the $[C_4H_6N_2]^{\cdot+}$ ions are able to protonate pyridine and not acetonitrile, and because these ions do not react with pyridine by charge exchange, the deprotonation energies of the ionized and distonic species and the ionization energies of neutral methylpyrazoles were also calculated. Copyright © 2000 John Wiley & Sons, Ltd.

KEYWORDS: pyrazole *N*-methylide radical cation; ion–molecule reactions; mass spectrometry; DFT molecular orbital calculations

INTRODUCTION

The distonic pyridine *N*-methylide radical cation $\mathbf{1}^{\cdot+}$ has been extensively studied in recent years.[1–4] General methods of production were based on the transfer of ionized methylene ($CH_2^{\cdot+}$) to neutral pyridine by using various experimental methods, such as chemical ionization[1,2] and ion-molecule reactions in a pentaquadrupolar instrument[3] or in a Fourier transform ion cyclotron resonance spectrometer.[2] Dissociative ionization of the stable betaine **2** was another convenient source for $\mathbf{1}^{\cdot+}$ ion production under electron ionization conditions (Scheme 1).

Some ions analogous to $\mathbf{1}^{\cdot+}$ have also been generated by transfer of $CH_2^{\cdot+}$ (from ionized oxacyclopropane) to pyrazole: the distonic structure $\mathbf{3}^{\cdot+}$ (denoted **a** hereafter) has been proposed on the basis of collisional activation experiments.[5,6] The molecular ions of *N*-acetylpyrazole (**4**) have been shown to undergo decarbonylation upon electron ionization and the distonic structure $\mathbf{3}^{\cdot+}$ (**a**) has been proposed (see Scheme 2) for these fragment ions.[7,8]

In the present work, the $[\mathbf{4}\text{-CO}]^{\cdot+}$ ions were reinvestigated by using ion–molecule reactions in a new hybrid mass spectrometer of sectors–quadrupole–sectors configuration (see Experimental Details section). The reactivity of these ions **a** with some neutral species was compared with that of reference ions, namely the molecular ions of the 1-methyl-, 3(5)-methyl- and 4-methylpyrazoles **5–7** and ions **b** which can be the ions resulting from $CH_2=NH$ loss from ionized 3(5)-dimethylaminopyrazole (**8**) (see Scheme 3). The forma-
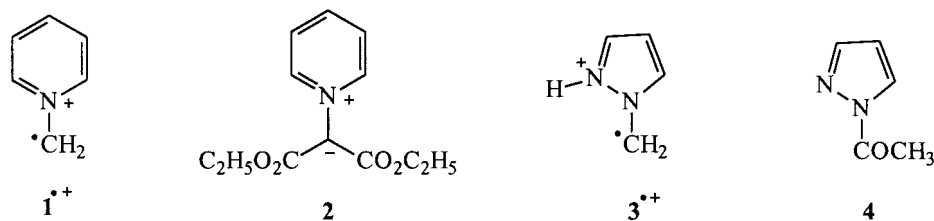
Scheme 1
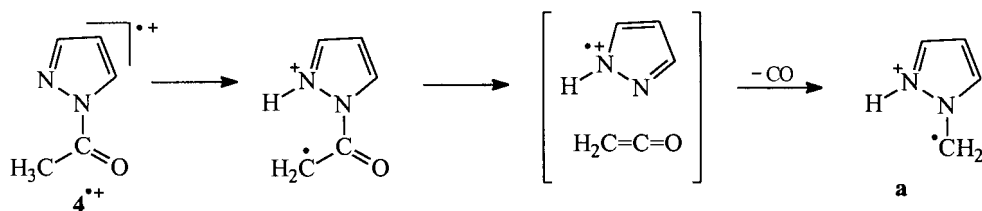
Scheme 2
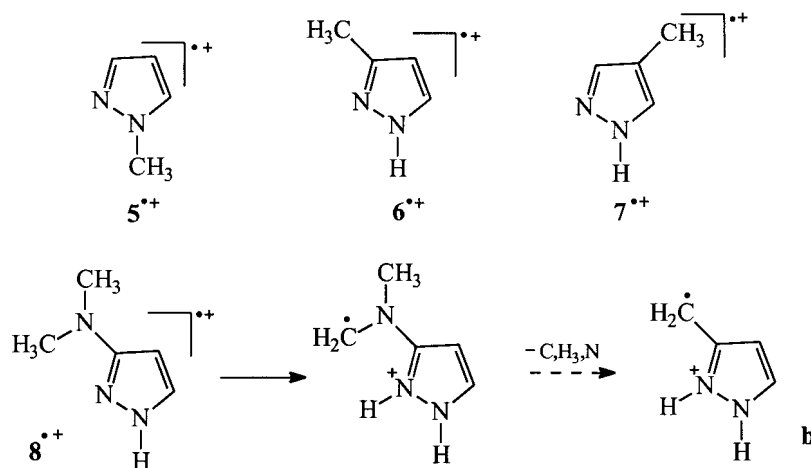
Scheme 3

tion of **b** ions from **8**$^{\cdot+}$ is proposed by analogy with the case of ionized 2-(*N,N*-dimethylamino)pyridine which generates the tautomer of ionized 2-picoline by losing CH$_2$=NH.[4]

EXPERIMENTAL RESULTS

Collisional activation at low kinetic energy

Before discussing the nature of the ion–molecule products between the [C$_4$H$_6$N$_2$]$^{\cdot+}$ ions and various neutral reagents, we will first describe the results of collisional activation (CA) with argon in the low kinetic energy regime (*ca* 20–30 eV). The relative abundances of the fragment ions, excluding *m/z* 81 (loss of H$^\cdot$, base peak in all cases), which is by far the most intense unimolecular dissociation, are collected in Table 1.

A common fragmentation yields *m/z* 55 ions. This loss

of CHN is already detected even in the absence of the collision gas and may therefore imply a rearrangement reaction before cleavage. Although important intensity differences are seen in these CA spectra, significant structural information arises only from the presence of

Table 1. CA (argon) mass spectra [*m/z* and relative intensities (%)] of the [C$_4$H$_6$N$_2$]$^{\cdot+}$ ions[a]

Ion	*m/z*											
	68	67	56	55	54	53	52	42	41	40	39	28
a	7	—	—	100	94	47	19	18	9	—	—	5
b	—	38	16	100	5	—	—	51	5	—	5	—
5$^{\cdot+}$	—	—	—	79	68	19	9	100	12	10	5	—
6$^{\cdot+}$	—	5	5	100	61	54	—	32	13	6	—	—
7$^{\cdot+}$	—	—	—	100	58	8	—	—	—	—	—	5

[a] Spectra of **a** and **b** ions generated by (dissociative) ionization of **4** and **8**, respectively, are also included. Peaks of intensity less than 5% are disregarded.
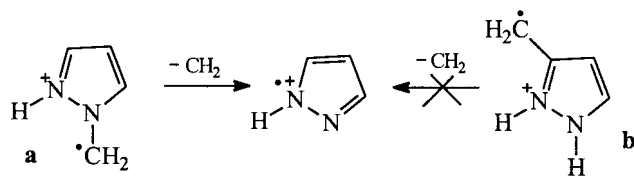
Scheme 4

m/z 67 and 68 ions. A loss of 14 Da (CH_2) is only present in the case of the $[C_4H_6N]^{\cdot+}$ ions derived from **4** (ions **a**). This fragmentation has also been detected in the CA spectrum at high kinetic energy, reported previously.[8] It is worth noting that the *m/z* ion 68 is not present in the case of the $[M-CH_2NH]^{\cdot+}$ ions of **8** (ions **b**), the losses of 15, 26 and 40 Da being instead the major fragmentation processes (Scheme 4).

From these results, we can conclude that the loss of a methylene (CH_2) from ions **b** would be a process energetically higher than that arising from ions **a** or even that ions **b** generated from $8^{\cdot+}$ do not have the distonic structure proposed in Scheme 4.

Ion–molecule reactions with nitric oxide

Nitric oxide has been used in some cases for the characterization of distonic or distonic-like species. In fact, several reactions have been observed, namely (a)
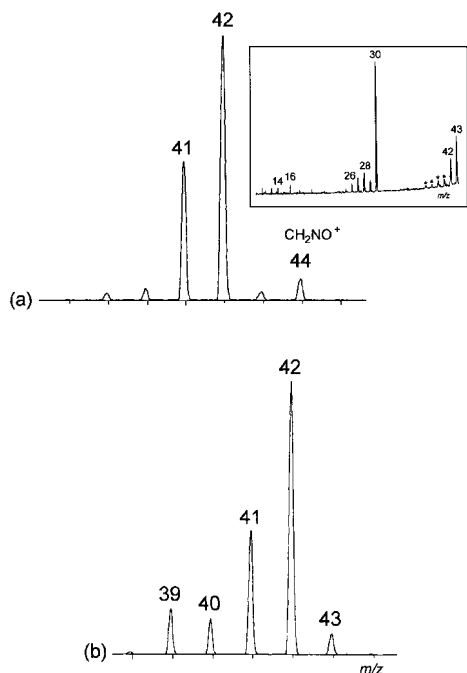
formation of CH_2NO^+ ions (*m/z* 44) from $\cdot CH_2-X^+-R$ ions,[9] (b) formation of XNO^+ ions (X = S, Se) from $R-C\equiv N^+-X^\cdot$ ions[10,11] and (c) formation of $[M + NO]^+$ cations.[12]

In Fig. 1, we present parts of the mass spectra of the ions produced in the r.f.-only quadrupole collision cell between decelerated *m/z* 82 ions (**a** or **b**) and nitric oxide. Only in the specific case of the ions **a** does a peak at *m/z* 44 corresponding to CH_2NO^+ ions appear. This peak, which is not observed for ions **b** or for the conventional $5^{\cdot+}$ and $6^{\cdot+}$ ions, confirms the presence of the CH_2 moiety in **a**, and therefore its distonic character. Although the intensity of the *m/z* 44 peak was very low (less than 0.5% of the most intense CA peak at *m/z* 55), we succeeded in recording the high-energy CA spectrum of these ions, which is shown as an inset in Fig. 1 (a). The base peak at *m/z* 30 for NO^+ ions clearly indicates that these ions result from the transfer of an ionized methylene to nitric oxide. This spectrum is moreover almost identical with that of the *m/z* 44 ions generated by reacting ionized cyclopropane with nitric oxide.

Ion–molecule reactions with dimethyl disulphide

Stirk *et al.*[13] have shown that dimethyl disulphide (DMDS) can efficiently indicate the distonic nature of radical cations. The distonic ions frequently react by methylthio radical abstraction. In contrast, their isomeric conventional structures react preferentially by charge exchange,[13] when such transfer is of course allowed by the ionization energies.

All the $[C_4H_6N_2]^{\cdot+}$ ions studied in this work react mainly with DMDS by charge exchange, producing very intense peaks at *m/z* 94 for $CH_3SSCH_3^{\cdot+}$ ions. For the distonic ions **a** and **b** additional smaller peaks are seen at *m/z* 129 corresponding to the abstraction of a $CH_3S^\cdot$ radical. This is exemplified in Fig. 2 in the case of the **b** ions.

After reacceleration at 8 keV, the *m/z* 129 ions were submitted to collisional activation and the fragments

Figure 1. Mass spectra (part) of the ions produced in the reaction of nitric oxide with ions (a) **a** and (b) **b**. The inset in (a) shows the CA (O_2) spectrum of the *m/z* 44 ions recorded in the linked scan mode. Peaks marked with asterisks are due to a not yet defined interference
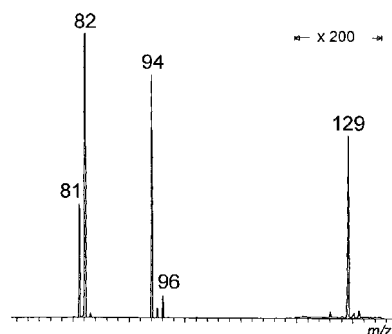

Figure 2. Mass spectrum (magnet scan) of the ions produced in the r.f.-only quadrupole collision cell after reaction of ions **b** with DMDS. The peak at *m/z* 82 is off-scale
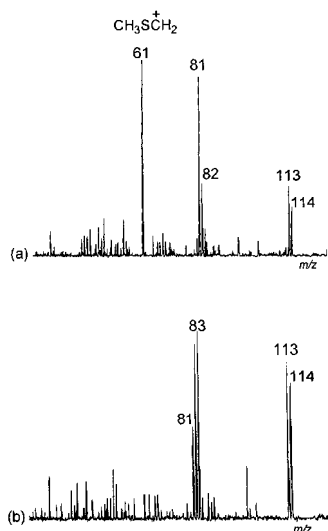
Figure 3. CA (O$_2$) spectra (linked-scan mode) of (a) the [**a** + CH$_3$S]$^+$ ions and (b) the [**b** + CH$_3$S]$^+$ ions (*m/z* 129)

collected by a linked scanning of the fields of the last three sectors (see Experimental Details section). The resulting spectra are shown in Fig. 3. Interestingly, the base peak of the [**a** + CH$_3$S]$^+$ ions is observed at *m/z* 61 for CH$_3$SCH$_2$$^+$ ions (loss of neutral pyrazole). These ions are not observed for the [**b** + CH$_3$S]$^+$ ions; instead, an intense loss of thioformaldehyde (*m/z* 83) is observed. The occurrence of a peak at *m/z* 61 is not expected in this last case as it should result in the elimination of a less stable ylid isomer of pyrazole (Scheme 5). Similar results have been obtained for pyridine *N*-sulphide (selenide).[14]

Ion–molecule reactions with dimethyl diselenide

It has been reported that dimethyl diselenide (DMDSe) is more efficient than DMDS concerning the determination of the distonic character of radical cations.[15] However, DMDSe is more difficult to handle owing to its lower vapour pressure. In addition, the large number of stable isotopes of selenium multiplies the peaks on the spectra, making interpretation difficult.

When experiments are performed using DMDSe, charge exchange is predominant (*m/z* 190, 100%) for all the [C$_4$H$_6$N$_2$]$^{\cdot+}$ ions, and abstraction of the CH$_3$Se$^\cdot$ radical is only observed for **a** and **b** ions (*m/z* 176, 4% and 2%, respectively), as expected on the basis of the results with DMDS.

Ion–molecule reactions with pyridine

The reactivity of the isomeric [C$_4$H$_6$N$_2$]$^{\cdot+}$ ions with pyridine was also studied in order to detect an eventual transfer of ionized methylene in the specific case of ions **a**. Apart from the spontaneous and collision-induced reactions (yielding mainly *m/z* 81 and 55 ions), the only reactivity observed is of a proton transfer giving protonated pyridine (*m/z* 80). Thus, all the [C$_4$H$_6$N$_2$]$^{\cdot+}$ isomers react as Brønsted acids with pyridine because of its high proton affinity [220.4 kcal mol^{-1} (1 kcal = 4.184 kJ)].[16] Since charge exchange is not observed, the ionization energy of the [C$_4$H$_6$N$_2$]$^{\cdot+}$ ions must be lower than that of pyridine (9.25 eV[17]).

The abundance ratios between the *m/z* 80 ions (protonation) and the *m/z* 81 (fragmentation) were measured to be between *ca* 0.2 and 0.8. Therefore, these ratios cannot be used for the characterization of the various isomers.

Ion–molecule reactions with acetonitrile

Compared with pyridine, acetonitrile has a reduced proton affinity (191 kcal mol^{-1}).[16] Therefore, it is expected that the proton transfer reaction could be disfavoured with respect to that of ionized methylene starting from ions **a**. In fact, acetonitrile *N*-methylide ions can be prepared by reacting distonic ions with acetonitrile, as has already been reported.[18]

Figure 4 shows parts of the mass spectra of the ions
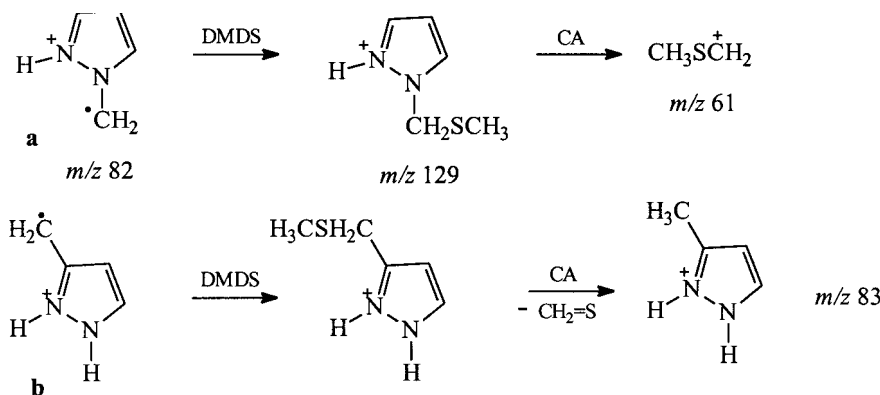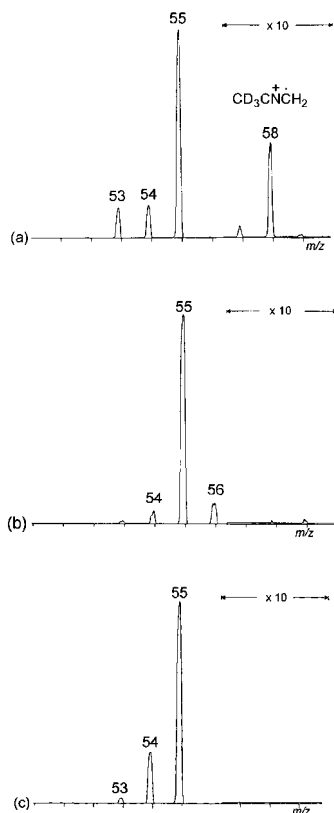

Scheme 5

Figure 4. Mass spectra (part) of the ions produced in the reaction of CD_3CN with ions (a) **a**, (b) **b** and (c) **5**$^{\cdot+}$

produced in the r.f.-only quadrupole collision cell when decelerated ions **a, b** or **5**$^{\cdot+}$ ions react with perdeuterated acetonitrile. The use of labelled acetonitrile is required in order to avoid interference between the ion–molecule product $CH_3CNCH_2^{\cdot+}$ and the collision-induced fragment (both C_3H_5N, *m/z* 55). Although of low intensity, a peak at *m/z* 58 ($CD_3CNCH_2^{\cdot+}$) is only seen in the case of ions **a**, again in agreement with their distonic character.

THEORETICAL RESULTS

In order to elucidate the experimentally observed reactivity, we performed DFT calculations using a basis set with sufficient flexibility to ensure reliable results.

Classical and distonic structures

The optimized geometries of the classical structures (**5**$^{\cdot+}$ and **6**$^{\cdot+}$) and their distonic counterparts (**a** and **b**) are displayed in Fig. 5. We also show the geometries of the transition states corresponding to 1,3-hydrogen transfer and which connect the aforementioned minima. The energies of these systems are presented in Table 2 at our highest level of calculation (including ZPE corrections).

The first conspicuous observation is that distonic forms are approximately 16 kcal mol^{-1} more stable than the

corresponding classical structures, the species **b** being about 10 kcal mol^{-1} more stable than **a**. The barriers for the formation of distonic ions from the classical structures are about 40 kcal mol^{-1}. The inverse barrier is about 60 kcal mol^{-1}. Thermodynamically, these values suggest an easier formation of distonic ions when starting from ionized species **5**$^{\cdot+}$ and **6**$^{\cdot+}$. The inverse reaction will then be more difficult.

The Mulliken analysis of distonic structures **a** and **b** reveals that the positive charges (see Scheme 6) are mainly concentrated in the carbon atoms. The unpaired electron is located by more than 80% over the carbon corresponding to the CH_2 moiety. The final structures can be described as the sum of the contributions of the different resonant forms presented in Scheme 6. From these descriptions we can see that ion **a** has a β- or γ-distonic character, contrasting with ion **b** which has only one minor γ-distonic form.

The absence in the CA spectrum of the **b** structure of a peak corresponding to the loss of CH_2 prompted us to analyse the relative energies of the products generated by such a loss. We can see in Table 2 that the dissociation energy for **a** will require 136.4 kcal mol^{-1} whereas in the case of **b** this value is 158.4 kcal mol^{-1}. An easier transfer of the CH_2 group in **a** than in **b** species is therefore expected, which is in accordance with the experimental results.

The carbenic ion c

Taking into account that the CA spectrum (see Table 1) shows a loss of 15 Da (assigned to a CH_3 loss), we can assume that the ion having the proposed structure **b** may isomerize into the classical ion **6**$^{\cdot+}$ before fragmenting, or even that this ion has other structures. This is supported by the fact that their respective CA spectra are different. We then considered the possible formation of a carbenic ion **c** which may also be generated from the precursor **8**$^{\cdot+}$, as depicted in Scheme 7. The stability of some heterocyclic carbenes has been convincingly demonstrated recently.[19]

The structure **c** is displayed in Fig. 5. This carbenic species is less stable than the distonic ion isomer **b** by 38.6 kcal mol^{-1}. The Mulliken analysis shows that the unpaired electron is almost entirely located at the carbenic carbon atom. The positive charge is shared between two carbon atoms, as shown in the relevant resonant forms displayed in Scheme 8.

The loss of a CH_3 radical starting from **c** could be favoured by the fact that it would make possible the ring resonance of the resulting cation.

Ionization energies

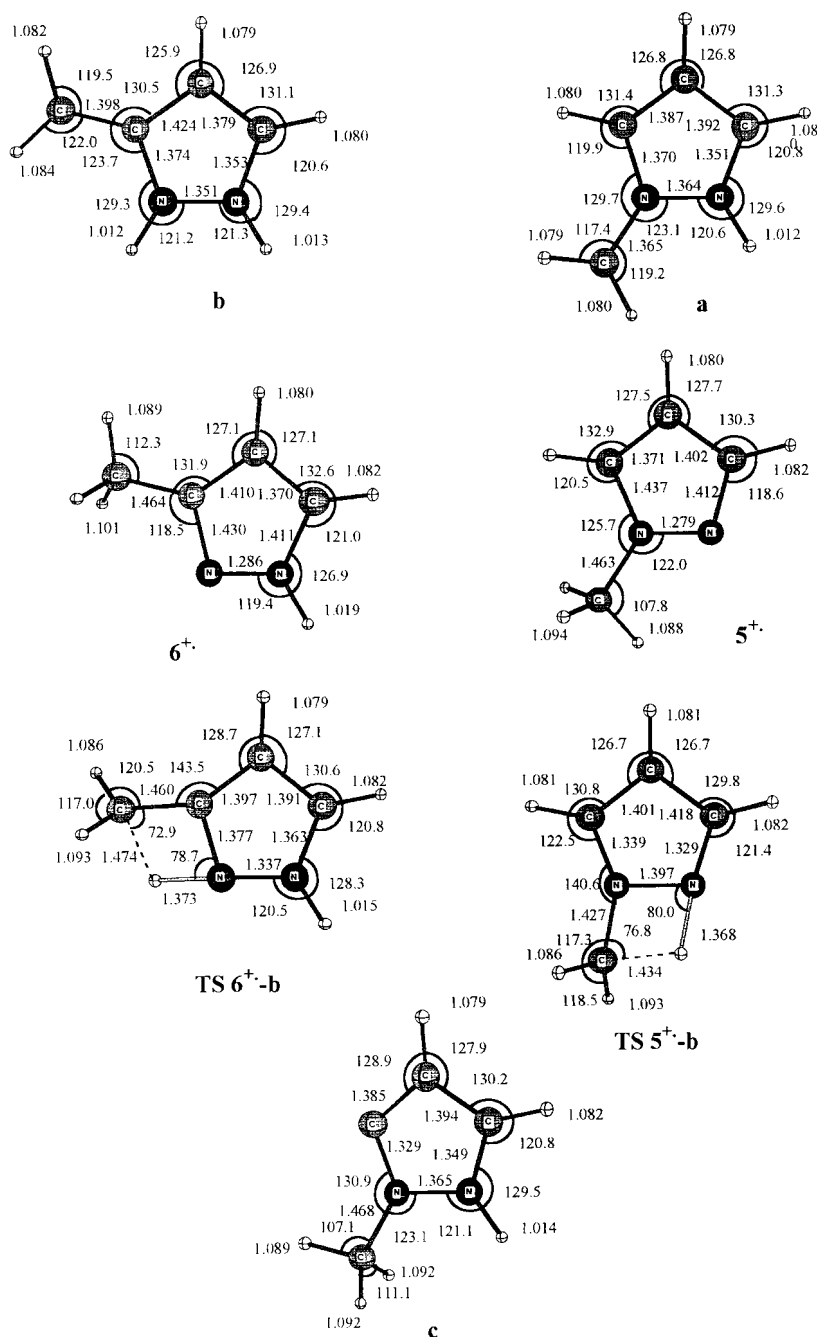In order to check the energetics involved in the possible

Figure 5. Optimized geometries of the $[C_4H_6N_2]^{\cdot+}$ ions. Bond lengths are given in ångstroms and bond angles in degrees

charge exchange reactions observed experimentally, we optimized, at the same level of theory, the corresponding neutral structures, **5, 6** and **13**. the species **14** that would correspond to the neutral form of the distonic species **a** will not be considered since it would have a diradical character. The ionization energies (*IE*s) of these species (presented in Table 2) were estimated, at the highest level of theory used, to be around 8.8 eV. These values are lower than the ionization energy of pyridine (9.25 eV), in agreement with the experimentally not observed (see above) charge-transfer reaction between pyridine and the other species involved in this study.

From the structures displayed in Fig. 6, one can see that the ionization of **5** and **6** gives rise to a significant shortening of the N—N bond whereas the two adjacent C—N bonds are significantly elongated. The ionizations of **5** and **6** are also accompanied by the rotation of the methyl group.

The corresponding neutral form of **b**, namely the species **13**, is not a planar structure, the two N—H moieties are out of the plane and in a *trans* configuration, so the resonance effects concern only the carbon atoms, in contrast to what is observed for ion **b**, which is planar. In addition, we can note that the calculated *IE* (6.59 eV)

Table 2. Calculated B3LYP total energies (in hartrees) and relative energies (in kcal mol^{-1}), ionization energies (*IE*s in eV) of neutral compounds and proton affinities (*PA*s in kcal mol^{-1}) of radical species

Species	6–31G**	ZPE	6–311 + (3df,2p)	6–311 + (3df,2p) + ZPE	E_{rel} (kcal mol^{-1})	IE	PA
Ions							
b	−265.242100	0.098224	−265.320768	−265.222544	0.0		
a	−265.225606	0.097938	−265.304261	−265.206323	10.2		
c	−265.183318	0.099282	−265.260334	−265.161052	38.6		
5$^{\cdot+}$	−265.202396	0.097132	−265.278048	−265.180916	26.1		
6$^{\cdot+}$	−265.215214	0.097160	−265.291465	−265.194305	17.7		
TS6$^{\cdot+}$ − **b**	−265.140702	0.092347	−265.217829	−265.125482	60.9		
TS5$^{\cdot+}$ − **a**	−265.133174	0.092558	−265.209722	−265.117164	66.1		
b − CH$_2$	−225.857941	0.071208	−225.925587	−225.854379			
a − CH$_2$	−225.876373	0.069174	−225.942481	−225.873307			
Radicals							
11a	−264.874336	0.085447	−264.960898	−264.875451	0.0		217
11b	−264.878869	0.085507	−264.964863	−264.879356	−2.5		215
10	−264.862024	0.084702	−264.947988	−264.863286	7.6		215
9	−264.852754	0.083523	−264.935576	−264.852053	14.7		214
12	−264.823069	0.086166	−264.906861	−264.829605	34.3		213
Neutrals							
6	−265.530489	0.098952	−265.615695	−265.516743	0.0	8.77	
5	−265.522340	0.099087	−265.606733	−265.507646	5.7	8.89	
13	−265.473701	0.098693	−265.563063	−265.464370	32.9	6.59	
CH$_2$	−39.131752	0.016512	−39.149858	−39.133346			

is lower than those of **5** and **6**, reflecting its instability. This ionization energy being lower than the ionization energy of dimethyl disulphide (8.18 eV),[20] the observation of a charge-exchange process (see earlier) must be due to the occurrence of a mixture of structures in the dissociative ionization of dimethylaminopyrazole (**8**).

Proton affinities

Finally, because the ions **5**$^{\cdot+}$, **a** and **b** are able to protonate pyridine but not acetonitrile, we investigated the radical structures resulting from the possible loss of a proton from nitrogen atoms of these ions in order to evaluate the corresponding proton affinities (*PA*s). The values reported in Table 2 are in agreement with the

experimental findings; the *PA*s of all the radicals considered here are indeed surrounded by those of pyridine and acetonitrile. The structures of the radicals **9**$^{\cdot}$, **10**$^{\cdot}$, **11a**$^{\cdot}$ and **11b**$^{\cdot}$ are displayed in Fig. 7.

The deprotonation of ion **b** can give both radicals **11a**$^{\cdot}$ and **11b**$^{\cdot}$, the latter being more stable than **10a**$^{\cdot}$ by only 2.5 kcal mol^{-1}. The isomers **9**$^{\cdot}$ and **10**$^{\cdot}$ are less stable than **11a**$^{\cdot}$ by 14.7 and 7.6 kcal mol^{-1}, respectively. From the Mulliken analysis the unpaired electron is located in the CH$_2$ moiety for **10**$^{\cdot}$, **11a**$^{\cdot}$ and **11b**$^{\cdot}$. In the case of the radical **9**$^{\cdot}$, coming from the classical ionized ion **5**$^{\cdot+}$, the unpaired electron is shared between the carbon atoms composing the ring.

It is worth noting that, in all the ionized distonic and radical structures investigated in this study, neither the charge nor the radical is localized on nitrogen atoms.

Scheme 6

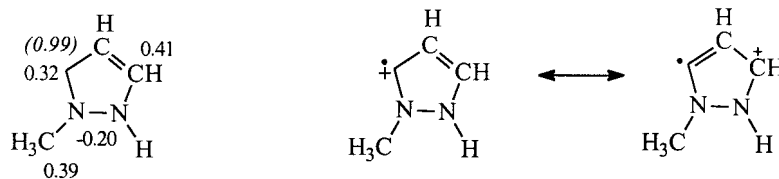**Scheme 7**

6

5
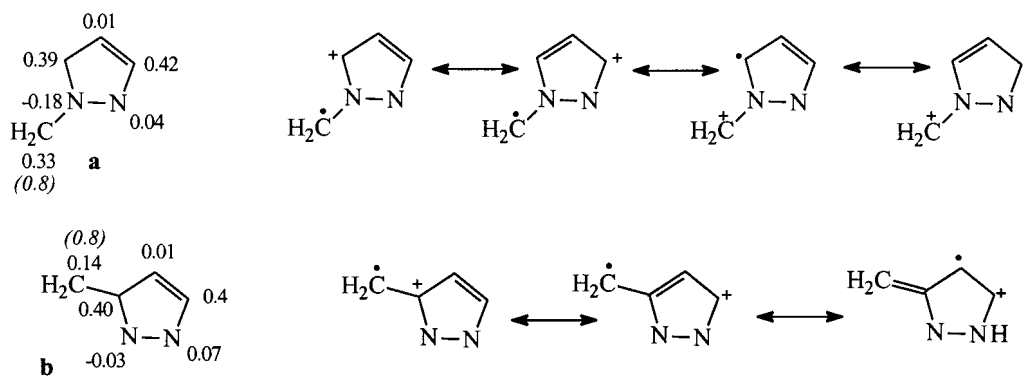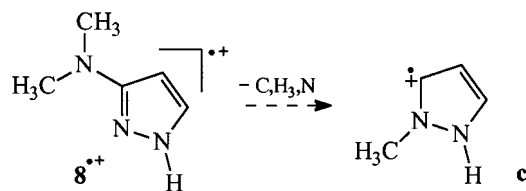
CONCLUSION

Although the reactivity of ions **a** toward the targets used in the present work is generally low, the results clearly indicate their distonic character, in excellent agreement with the CA data in the high or low kinetic energy regimes. In particular, ion–molecule reaction with dimethyl disulphide coupled with the high-energy CA spectrum of the ions produced by abstraction of $CH_3^·$ leaves little doubt about their pyrazolium *N*-methylide structure.

Formally, ions **b**, tautomers of 3-methylpyrazole, are not distonic ions. These ions are the most stable among the $[C_4H_6N_2]^{·+}$ species studied in the present work and are proposed to be produced in the dissociative ionization of dimethylaminopyrazole (**8**). The intense loss of 15 Da in the low-energy CA spectrum is nevertheless not yet understood and further experiments (*e.g.* an unambiguous synthesis of ions **c**) are required in order to clarify this peculiar behaviour. It is nevertheless worth noting that the tautomeric ion of 2-picoline behaves similarly.[21]

EXPERIMENTAL DETAILS

All the spectra were recorded on a large-scale tandem mass spectrometer[22] which has been recently modified to allow the study of ion–molecule reactions.[23] The spectrometer has been schematically presented elsewhere.[24] Briefly, it consists of a combination of sectors and an r.f. only quadrupole collision cell giving the sequence EBEqEBE (E = electric sector, B = magnetic sector and q = quadrupole collision cell). Typical conditions were accelerating voltage 8 keV, trap current 200 μA and ionizing electron energy 70 eV.
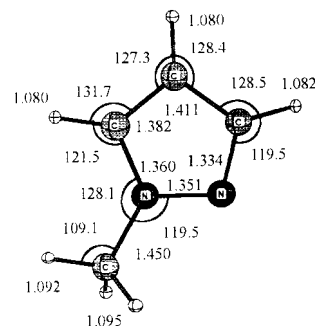
In the ion–molecule experiments, a beam of mass-selected ions (EBE) is decelerated to a few electron volts before entering the quadrupole collision cell in to which a neutral reagent is introduced at a pressure estimated as
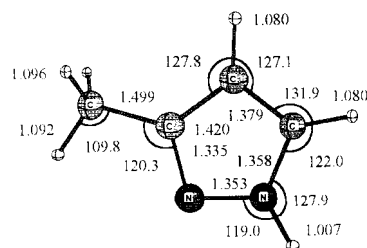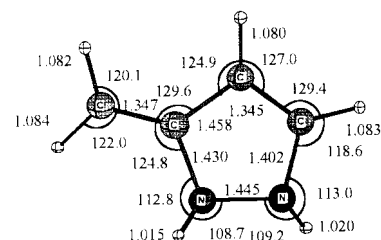

13

Figure 6. Optimized geometries of three $C_4H_6N_2$ neutrals. Bond lengths are given in ångstroms and bond angles in degrees

10^{-3} Torr (1 Torr = 133.3 Pa) The ion–molecule products, reaccelerated at 8 keV, can then be separated by scanning the field of the second magnet (B scan). Moreover, the high-energy CA spectra of the ions present in the quadrupole can be recorded by a linked scanning of the fields of the last three sectors (EBE, resolved mode) or a scanning of the field of the last electric sector after mass selection with the second magnet. In these CA experiments, a collision gas is introduced into cells
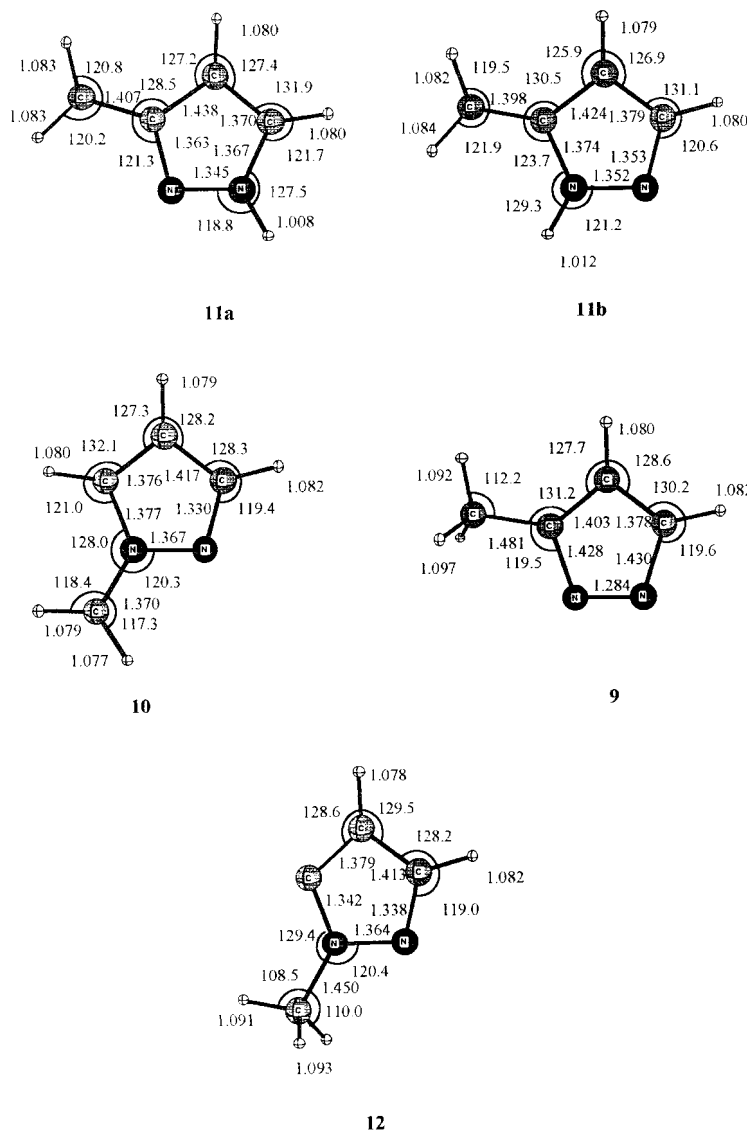

Scheme 8

Figure 7. Optimized geometries of the $C_4H_5N_2$ radicals. Bond lengths are given in ångstroms and bond angles in degrees

situated in front of the third and the fourth electric sectors.

The samples were commercially available (Aldrich) or prepared according to literature procedures (4^{25} and 8^{26}).

THEORETICAL DETAILS

The theoretical treatment of the different systems included in this work was performed by using the B3LYP density functional approach in the Gaussian-94[27] series of programs. The B3LYP approach is a hybrid method which includes the Becke's three-parameter non-local exchange potential[28] with the non-local correlation functional of Lee, Yang and Parr.[29] This method has been found to be fairly reliable as far as the description of closed- or open-shell species is concerned.[30] The geometries of the different species under consideration were optimized using the 6–31G (d,p) basis set. The harmonic vibrational frequencies of the different stationary points of the potential energy surface (PES) were calculated at the same level of theory as used for their optimization in order to identify the local minima and the transition states (TS) and to estimate the corresponding zero point energies (ZPE).

In order to take into account possible shortcomings of the basis set used, the final energies of the different species under study were obtained in B3LYP/6–311 + G(3df,2p) single-point calculations at the aforementioned B3LYP/6–31G(d,p) optimized geometrices.

REFERENCES

1. C. G. De Koster, J. J. van Houte and J. van Thuijl, *Int. J. Mass Spectrom. Ion Processes* **134**, 1–10 (1994).
2. S. J. Yu, M. L. Gross and K. R. Fountain, *J. Am. Soc. Mass Spectrom.* **4**, 117–124 (1993).
3. F. C. Gozzo and M. Eberlin, *J. Am. Soc. Mass Spectrom.* **6**, 554–563 (1995).
4. R. Flammang, O. Thoelen, C. Quattrocchi and J. L. Bredas, *Rapid Commun. Mass Spectrom.* **6**, 135–139 (1992).
5. P. Boulanger, PhD Thesis, University of Mons-Hainaut (1996).
6. C. G. De Koster, J. J. van Houte and J. van Thuijl, *Int. J. Mass Spectrom. Ion Processes* **123**, 59 (1993).
7. A. Maquestiau, Y. Van Haverbeke, R. Flammang, R. M. Claramunt and J. Elguero, *Bull. Soc. Chim. Fr.* 2693–2695 (1975).
8. A. Maquestiau, A. Tommasetti, C. Pedregal-Freire, J. Elguero and R. Flammang, *Bull. Soc. Chim. Belg.* **93**, 1057–1066 (1984).
9. T. Weiske, H. van der Wel, N. M. M. Nibbering and H. Schwarz, *Angew. Chem., Int. Ed. Engl.* **23**, 733–734 (1984).
10. P. Gerbaux and R. Flammang, unpublished results.
11. P. Gerbaux, R. Flammang, E. H. Mørkved, M. W. Wong and C. Wentrup, *Tetrahedron Lett.* **39**, 533–536 (1998).
12. R. Flammang, V. Sciammana and P. Gerbaux, unpublished results.
13. K. M. Stirk, J. C. Orlowski, D. T. Leeck and H. I. Kenttämaa, *J. Am. Chem. Soc.* **114**, 8604–8606 (1992).
14. (a) P. Gerbaux, Y. Van Haverbeke and R. Flammang, *J. Mass Spectrom.* **32**, 1170–1178 (1997); (b) P. Gerbaux, Y. Van Haverbeke and R. Flammang, *Int. J. Mass Spectrom.* **184**, 39–47 (1999).
15. K. Thoen, B. J. Beasley, R. L. Smith and H. I. Kenttämaa, *J. Am. Soc. Mass Spectrom.* **7**, 1245–1250 (1996).
16. D. H. Aue and M. T. Bowers, in *Gas Phase Ion Chemistry*, edited by M. T. Bowers, Vol. **2**. Academic Press, New York (1979).
17. S. G. Lias, J. E. Bartmess, J. F. Liebman, J. L. Holmes, R. D. Levin and G. Mallard, *J. Phys. Chem. Ref. Data* **17**, Suppl. 1 (1988).
18. P. Gerbaux, R. Flammang, M. T. Nguyen, J. Y. Salpin and G. Bouchoux, *J. Phys. Chem. A* **102**, 861–869 (1998).
19. (a) D. J. Lavorato, J. K. Terlouw, T. K. Dargel, W. Koch, G. A. McGibbon and H. Schwarz, *J. Am. Chem. Soc.*, **118**, 11898–11904 (1996); (b) G. A. McGibbon, J. Hrusak, D. J. Lavorato, H. Schwarz and J. K. Terlouw, *Chem. Eur. J.* **3**, 232–236 (1997); (c) G. A. McGibbon, C. Heinemann, D. J. Lavorato and H. Schwarz, *Angew. Chem., Int. Ed. Engl.* **36**, 1572–1575 (1997); (d) D. J. Lavorato, J. K. Terlouw, G. A. McGibbon, T. K. Dargel, W. Koch and H. Schwarz, *Int. J. Mass Spectrom. Ion Processes* **179/180**, 7–14 (1998).
20. C. Y. Ng, in *The Structure, Energetics and Dynamics of Organic Ions*, edited by T. Baer, C. Y. Ng and I. Powis. Wiley, New York (1996).
21. P. Gerbaux, PhD Thesis, University of Mons-Hainaut (1999).
22. R. H. Bateman, J. Brown, M. Lefevere, R. Flammang and Y. Van Haverbeke, *Int. J. Mass Spectrom. Ion Processes* **115**, 205–218 (1992).
23. R. Flammang, Y. Van Haverbeke, C. Braybrook and J. Brown, *Rapid Commun. Mass Spectrom.* **9**, 795–799 (1995).
24. P. Gerbaux, Y. Van Haverbeke, R. Flammang, M. W. Wong and C. Wentrup, *J. Phys. Chem. A* **101**, 6970–6975 (1997).
25. S. Iwazaki, *Helv. Chim. Acta* **59**, 2738 (1976).
26. H. J. Gay, K. Hafner and M. Nevenschwander, *Helv. Chim. Acta* **52**, 2641 (1969).
27. M. J. Frisch, G. W. Trucks, H. B. Schlegel, P. M. W. Gill, B. J. Johnson, M. A. Robb, J. R. Cheeseman, T. A. Keith, G. A. Peterson, J. A. Montgomery, K. Raghavachari, M. A. Al-Laham, V. G. Zakrzewski, J. V. Ortiz, J. B. Foresman, J. Cioslowski, B. B. Stefanow, A. Nanayaklara, M. Challacombe, C. Y. Peng, P. Y. Ayala, W. Chen, M. W. Wong, J. L. Andres, E. S. Replogle, R. Gomperts, R. L. Martin, D. J. Fox, J. S. Binkley, D. J. Defrees, J. Baker, J. P. Stewart, M. Head-Gordon, C. Gonzalez and J. A. Pople, Gaussian 94. Gaussian, Inc. Pittsburgh, PA (1995).
28. (a) A. D. Becke, *J. Chem. Phys.* **98**, 5648–5652 (1993); (b) A. D. Becke, *J. Chem. Phys.* **96**, 2155–2160 (1992).
29. C. Lee, W. Yang and R. G. Parr, *Phys. Rev. B* **37**, 785–789 (1988).
30. (a) J. W. Gauld and L. Radom, *Chem. Phys. Lett.* **275**, 28–34 (1997); (b) A. Nicolaides, D. M. Smith, F. Jensen and L. Random, *J. Am. Chem. Soc.* **119**, 8083–8088 (1997); (c) M. W. Wong and L. Radom, *J. Phys. Chem. A* **102**, 2237–2245 (1998).